AUTOMATION AND ROBOTICS IN AGRICULTURE

CHAPTER 3: ROBOTICS FOR AGRICULTURAL SYSTEMS

3.1. Introduction

In agriculture, robotics has been increasingly adopted, in the last few years, to improve efficiency and productivity. Most of the research efforts have been applied to fresh market vegetables and fruit harvesting jobs, which are usually tiring, time-consuming, and specifically demanding. Harvest labor for many crops accounts for about one-half to two-thirds of the overall labor costs. Additionally, due to a decrease in the population of farmers, harvesting is expected to be automated.

Figure 3.1. Lettuce harvest technology

[Source: http://www.gemuesetechnik.de/hortus-salaterntetechnik.html?&L=4]

In applying robots to the variability of agricultural harvesting jobs, extensive research has been carried out: cucumbers, asparagus, tomatoes, apples, lettuce, citrus, oranges, grapes, strawberries, and strawberries. In (Arima et al., 2004; Brown, 2002; Edan et al., 2000; Hannan and Burks, 2004; Murakami et al., 1995; Peterson and Wolford, 2003b; Van Henten et al., 2002) some distinguished examples of agricultural robotic systems can be found. In recent years, Specific work on robotics for agricultural tasks such as spraying, harvesting, berry thinning and transplanting has been established (Ling et al., 2004; Monta et al., 1992; Monta et al., 1998). For developing visual guidance system, computer vision has also been extensively employed in agriculture (Benson et al., 2003; Pilarski et al., 1999), grade judgment of fruits (Nagata and Cao, 1998), for weed control (2002; Downey et al., 2003; Jeon et al., 2005) and or fruit recognition on trees (Peterson et al., 2003a). Specific research on vision-based harvesting of melons can be found in (Dobrusin et al., 1992), asparagus in (Humburg and Reid, 1992), and of tomatoes in (Chi and Ling, 2004).

3.2. Radicchio Harvester

Aiming at both cost-effectiveness and efficiency, the robotic harvester was designed(Foglia and Reina, 2006). It comprises of a grippe and a double four-bar manipulator for the harvesting of radicchio. Radicchio needs a stem cutting of the plant about 10 mm under the soil surface, which is normally a 10–12 mm diameter stem and120 – 130 mm in diameter. Both gripper and manipulators are pneumatically actuated. Pneumatic actuators have a high power-weight ratio though compared to electric actuators they are difficult to control, which makes them appropriate for agricultural applications. Moreover, the design of the gripper is according to the pneumatic muscles, which on the other hand are robust, light, easy to maintain, and inexpensive. Good compliance with the plant is also provided by the pneumatic actuation due to the compressibility of air, which permits to recompense for small errors in the measurement of radicchio location in the field (Kondo and Ting, 1998; Antonelli et al., 2017).

3.2.1. Grippers

The following requirements should be fulfilled by all grasping devices: simplicity in the mechanical design, robustness, easy implementation, and low-cost (Solis-Salazar et al., 2008; Zion et al., 2014).

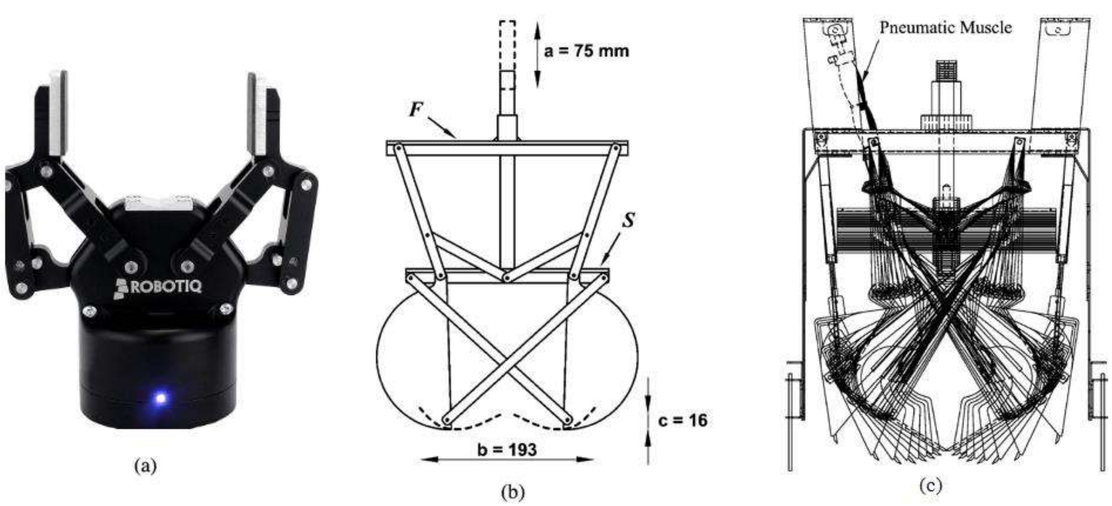

Figure 3.2. The two-finger gripper (a), and its cutting sequence (b)

[Source: https://wiredworkers.io/product/robitiq-2f-85/]

[Source: https://link.springer.com/chapter/10.1007%2F978-3-540-74027-8_27]

A two-finger gripper prototype has been shown in Figure 3.2 designed for agricultural application; it employes two bucket-like fingers featuring a linear blade attached to their tips to carry out cutting operation and it is made of aluminum with a total weight of about 16 kg. Two pneumatic muscles actuate the driving linkage which is linked between the vertical slider *S* and the fixed plate *F* as specified in Fig.3 2(a, b); with symmetrical behavior, the two fingers operate simultaneously. Observe that the vertical stroke *a* of the slider *S* transforms into a vertical and horizontal displacement of the denoted fingertips with *c* and *b* in Fig.3 2(a). In the same figure, the dashed line shows the fingertip paths. When all four boundary switches touch the soil, the closure of the gripper starts. Then, at about 10 mm underground the fingers cut the stem and at the same time pull the plant out of the terrain as displayed in Fig.3 2(b) during the complete operation by the successive configurations of the gripper (Kelc et al., 2019).

A three-finger gripper was also considered, to increase manipulation ability. It is shown in Fig.3 3 by the use of pneumatic muscles actuating three bucket-like fingers independently and a four-bar mechanism for driving, which permits performing the needed stem cutting at around 13 mm underground. This is displayed in the Fig.3 3(b) by the series of cut trailed by one of the fingers. Note that the fingers are located at 120° and the height of the higher support for the muscles, signified with *B* in Fig.3 3(b) can be moved to regulate the relationship between the displacement of the fingertip and the pneumatic muscle stroke (Milella et al., 2004; 2006).

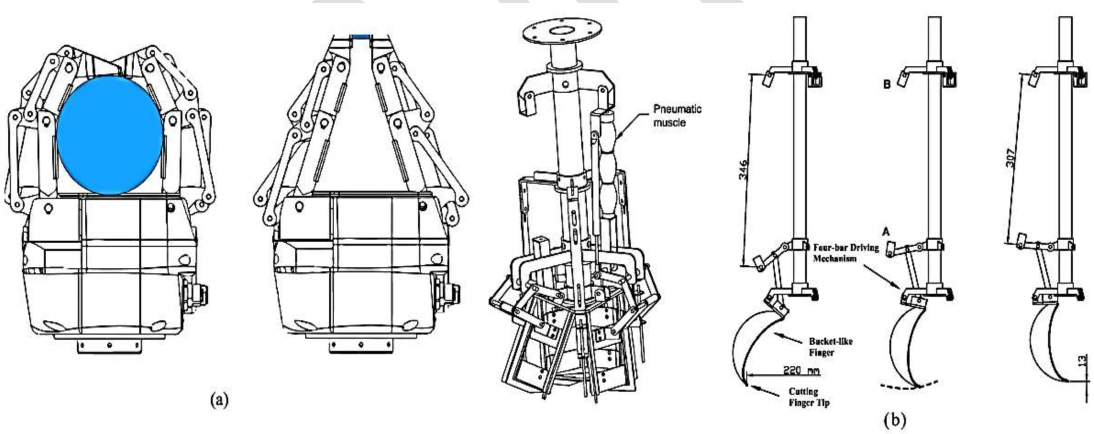

Figure 3.3. The three-finger gripper (a), and its cutting sequence (b)

[Source: https://www.wevolver.com/wevolver.staff/3-finger.adaptive.robot.gripper/master/blob/Overview.wevolver]

3.2.2. Manipulator

To approach the plant, deliver the radicchio to a container on the carrier, and perform the harvesting task, the mobility to the gripper is provided by the manipulator.

Following are the requirements for the manipulator design: along the field lines, the displacement between the plants of about 700 mm, the speed of about 0.4 km/h of the carrier (tractor) of the robotic harvester, and the required minimum height of 800 mm from the ground by the CCD camera attached to the gripper in the field for efficient identification of the plant during the targeting stage. The basis of the architecture of the manipulator is on four-bar parallel links, which permit the gripper to stau level. Three applicant configurations are examined that use one, two, and three pneumatic actuators as shown in the functional schemes displayed in Fig.3 5. A moving delivery tray is used in all solutions reduce the harvesting cycle time. Normally, the number of independent degrees of freedom of the end-effector corresponds to the number of actuated degrees of motions of a manipulator. The more degrees of motions, the higher cost of the manipulator, and the higher the degree of flexibility (Sciavicco and Siciliano, 2000). Robot for sweet-pepper harvesting is shown in Fig. 3.4.

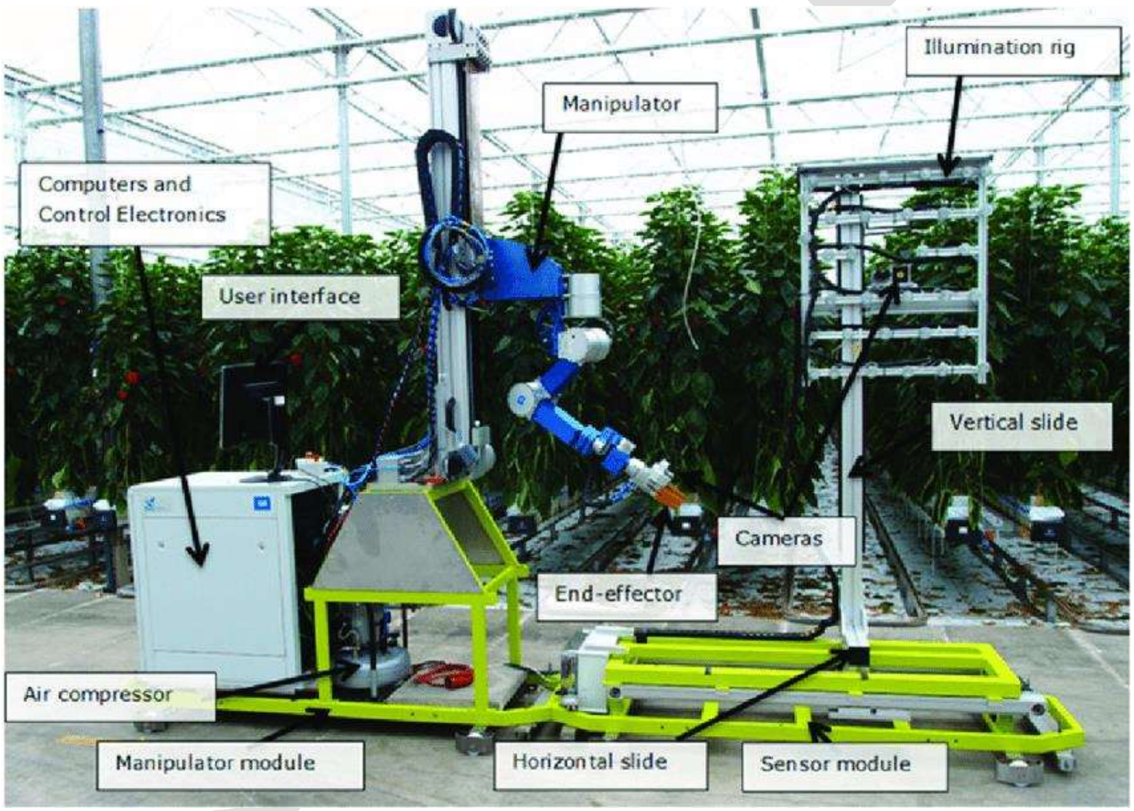

Figure 3.4. Robotic setup for sweet-pepper harvesting

[Source: https://www.researchgate.net/figure/Final-integrated-robot-for-harvesting-sweet-pepper-fruit-as-used-for-the-greenhouse_fig10_281536425]

The one-actuator architecture (Fig.3 5(a)) is less versatile but allows the lowest costs; hence, the best trade-off has been resulted by the two-actuator configuration (Fig.3 5(b)) and has been selected for this system. A characteristic harvesting cycle path has been shown in Figure 3.5 followed by the gripper with the two-actuator manipulator. To a ground reference frame in Fig.3 6(a), the same path is referred and to a coordinate system embedded with the carrier in Fig.3 6(b). Until the plant is localized by the vision-based module, the gripper moves forward horizontally (point *B*' in Fig.3 6(a, b)).

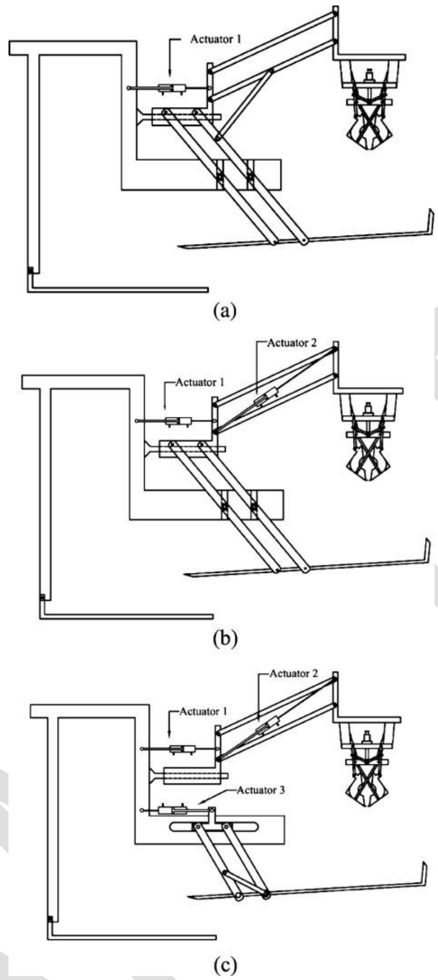

Figure 3.5. Four bar-based manipulator employing: one (a), two (b), and three actuators (c)

[Source: https://link.springer.com/chapter/10.1007%2F978-3-540-74027-8_27]

Then, towards the plant (point *C*), the gripper starts its downward course, where it carries out the cutting operation and concerning the ground keeping null velocity. The return of the gripper towards the starting configuration has been marked by point *D* where the system can start the cycle again as the plant is dropped on the delivery tray (point *E*).

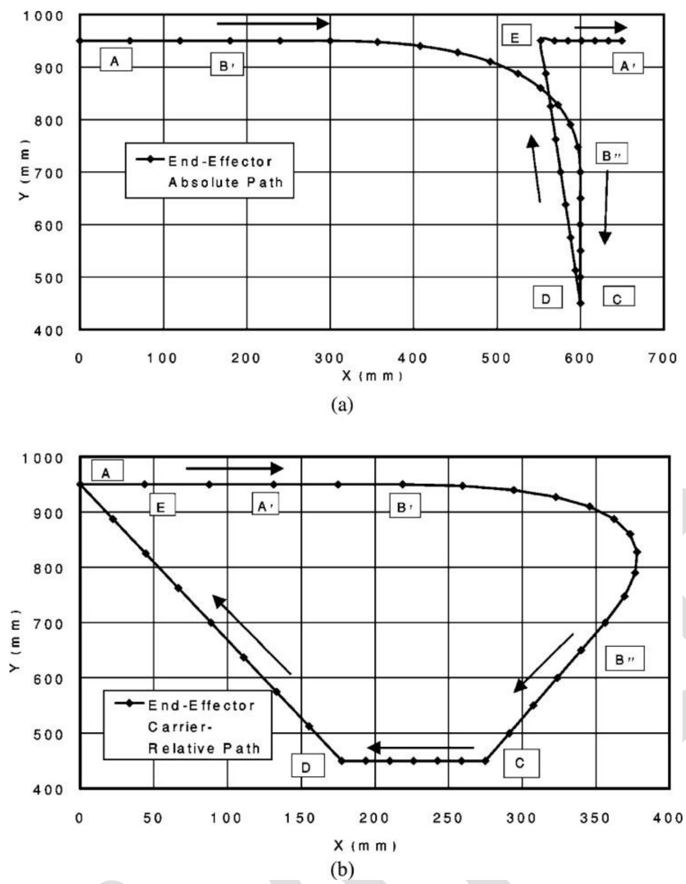

Figure 3.6. Harvesting cycle expressed in terms of the path of the end-effector concerning a ground frame (a), and to a carrier-embedded coordinate system (b)

[Source: https://link.springer.com/chapter/10.1007%2F978-3-540-74027-8_27]

3.2.3. The Radicchio Visual Localization

To localize and detect the plants in the field, a vision-based algorithm was established; the basis of the RVL module morphological operations and intelligent color filters, which permit one to distinguish the radicchio within the images clutched by a CCD color camera with a frame rate of 5 Hz straddling on the end-effector.

Normally, the following steps are included in the algorithm:

1. To enhance the thresholding operation, image acquisition in the Hue Saturation Luminance (HSL) space as described below (Fig.3 7(b)).
2. To obtain two images, Hue and Luminance plane extraction where the radicchio is physically separate from the surrounding (Fig.3 8).
3. To obtain two binary images, independent thresholding in the Luminance and Hue planes comprising the radicchio white pixels and purple pixels respectively (Fig.3 9). By analyzing the histogram of the

two planes, the thresholds are experimentally determined. Particularly, the threshold for the Hue plane was found to be well defined as:

$$\frac{T_{Max} + T_{Min}}{2} \qquad (1)$$

where T_{min} and T_{max} are the minima and maximum intensity values respectively. The threshold for the Luminance plane is set, as the highest value of grey levels as the white parts of the plant related to the pixels with the largest luminance.

4. To combine the information into a unique image, Or-operation of the two images (Fig.3 10(a)).
5. Particle and morphological filtering(Fig.3 10(b)). Particularly, a morphological opening is applied using a 5×5 pixels substructure to remove isolated background pixels and open up touching futures i.e., an operation of erosion followed by dilation. Then, objects with an area are filtered out, i.e., a total number of pixels, smaller than a threshold value (2000 pixels). Lastly, a morphological closing, by bridging the remaining small gaps allows reconstructing the shape of the plant i.e., a succession of erosion and dilation.
6. Convex hull production of the extracted feature (Fig.3 11(a)).
7. Description of the minimum enclosing circle (Fig.3 11(a)), i.e. the minimum circle which encircles the extracted set of points (Xu *et al.*, 2003). This geometrical algorithm assistances to notice the plant even when only a comparatively small uncentered part of the radicchio is extracted.

The overall result of the localization algorithm is shown in Figure 3. 11(b). Over the original image, the minimum enclosing circle is overlaid with its center representing the coordinates of the centroid of the plant in the image reference frame.

Figure 3.7. Sample image of the radicchio in the RGB (a), and HSL (b) color space

[Source: https://www.istockphoto.com/ae/photo/leaves-and-cabbageheads-of-red-radicchio-isolated-gm1172776579-325489497]

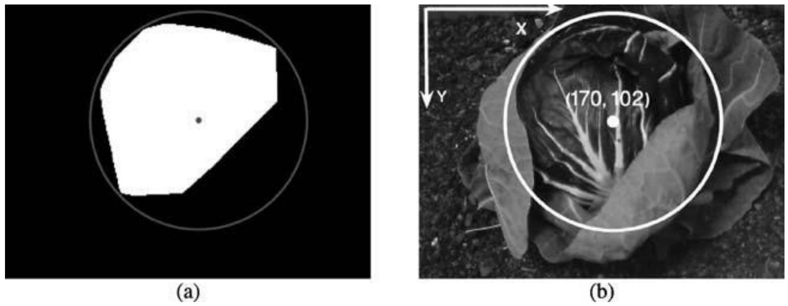

Figure 3.8. Convex hull and minimum enclosing circle generation (a), radicchio localization in the image plane (b)

[Source: https://link.springer.com/chapter/10.1007%2F978-3-540-74027-8_27]

3.3. Fennel Cutting System

A robotic system for the automated cut of just-harvest fennel wandering at high speed without any preordered alignment on a conveyor has been described in this section. During the post-harvest process of fennel, this operation is usually essential to generate ready-to-market products (Foglia et al., 2005; Ahmed et al., 2016). To enhance the quality of the final product and manufacturing rate, an automated cutting device would be helpful.

3.3.1. Cutting Mechanism

The proposed mechanism consists of two four-bar linkage cutters and is shown in Fig.3 9, so-called fore and backing cutter respectively, which function long the same path asynchronously that is shown by a black solid line in Fig.3 9. Between the two cutters, the time delay is proportional to the required length of the funnel as

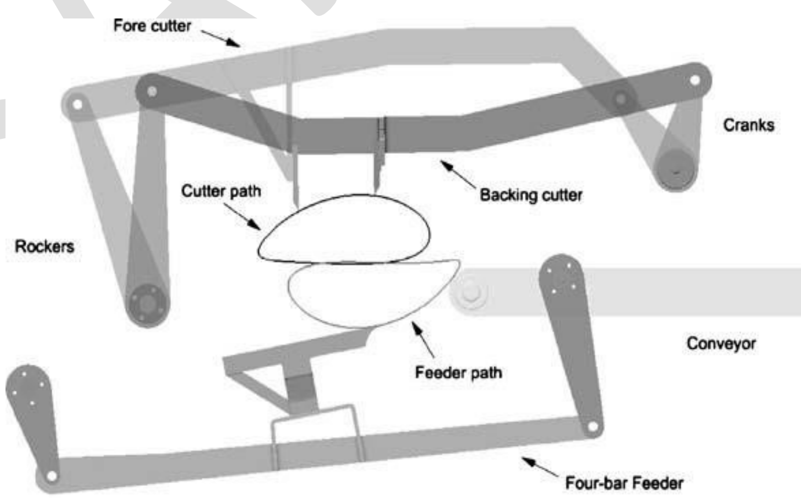

Figure 3.9. The mechanism for automated cutting of just-harvest fennel

[Source: https://link.springer.com/chapter/10.1007%2F978-3-540-74027-8_27]

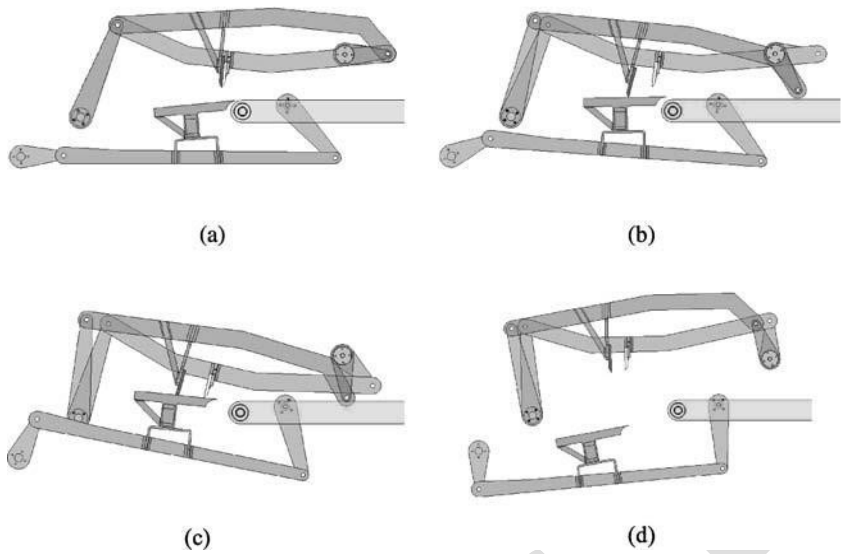

Figure 3.10. Configurations of the mechanism during a typical cutting cycle: starting configuration (a), first cut performed by the fore cutter (b), second cut performed by the backing cutter (c), and return of the two cutters to the starting configuration as the r

[Source: https://link.springer.com/chapter/10.1007%2F978-3-540-74027-8_27]

proposed by the identification module defined later in this section. The plant from the conveyor is picked up by the third four-bar linkage feeder and delivers the needed support to carry out a double cutting operation. Observe that during the cutting stage the feeder and cutter follow about a straight line giving a strong and stable cutting action. Some typical configurations of the mechanism have been shown in Figure 3.8 during its working cycle (Anubhuti et al., 2011).

3.3.2. The Fennel Visual Identification

Fennels traveling at high speed on a conveyor are processed by the FVI system detecting the parts of the plant, such as leaves and root, and to produce a high-quality market product it needs to be cut off. In Fig.3 11 are shown, the final market product and the just-harvest fennel covered the cutting lines) delivered by the FVI module. The FVI module operates in real-time with a processing rate of 60–80 plants per minute and a sampling rate of 10 Hz. Usually, the following steps are included in the algorithm (Milella *et al.*, 2006):

1. RGB to HSL conversion and image acquisition.
2. By processing the Hue plane, extraction of the plant from the image.
3. Individuation of the alignment of the plant on the conveyor.
4. For the cutting operation, the calculation of appropriate lines.

Each step is discussed in detail in the remainder of this section.

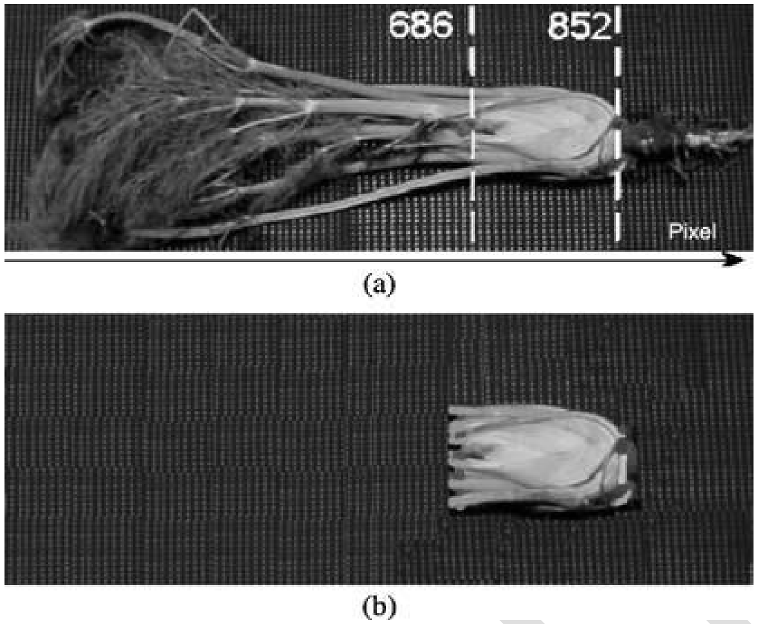

Figure 3.11. The FVI module establishes the cutting lines (a) to produce the ready-to-market fennel (b)

[Source: https://link.springer.com/chapter/10.1007%2F978-3-540-74027-8_27]

Image conversion in the HSL space – Instead is using RGB, the use of HSL space permits differentiating between luminance and color information, hence enhancing the successive image segmentation.

Hue plane processing – Using thresholding in the Hue plane, the fennel can be effortlessly differentiated from the belt background by the related histogram. Through an initial calibration, the threshold value is experimentally determined. At the beginning of the process, an image of the belt is attained, without any fennel and the threshold for segmentation is fixed as μ-3σ where σ and μ are respectively, the standard deviation and the mean of the distribution of the grey levels of the hue image of the belt. The pixels of the plant can be designated and the grey levels of the belt are insulated. Then, joining connected pixels and eliminating isolated pixels can be performed by an appropriate combination of dilation and erosion operations to gain a unique object demonstrating the fennel (Artés et al., 2002).

Individuation of the plant orientation and cutting lines –it is essential to know the orientation of the plant, for the FVI to work correctly. Two approaches are adopted and are discussed below. The first approach aims to detect the relative position between the so-called "green" and "white" parts of the plant. By thresholding in the saturation plane, the *green* part can be detected, since it links to the pixels with the maximum intensity values in this plane.

Similarly, by thresholding in the luminance plane, the *white* part of the plant can be isolated, since this part is made up of pixels with the maximum intensity values in this plane. It is possible to derive the orientation of the plant by comparison of the position of the centroid of the green part with that of the white part. Then, considering both orientation and dimension of the plant, the cutting lines can be fixed. Particularly, either the right side or the left side of the bounding box, the rooted cutting line will be fixed according to the plant orientation, contouring the *white* part; at a distance from the root cutting line of two-thirds of the box length, the cutting line to removing the leaves is set (Escalona et al., 2005; Gao & Wang, 2011).

Based on color matching techniques, the second approach for approximation of the plant orientation is developed combined with the greyscale pattern matching. This method typically depends on the normalized cross-correlation approach. for the upper leaves and the root, two templates are defined respectively which will serve as masks. Each template is stimulated around the image approximating the value of the normalized correlation coefficient whose peak signifies the location of the best matches in the image of the mask (Masuhr & Menzel, 1972; Sacchetti et al., 2003).

3.4. Experimental Applications of Agricultural Robotics

Field and experimental results are acquired by Foglia et al. (2008) are presented in this section to asses their performance in terms of repeatability, accuracy, variations in lighting and robustness to disturbances, obtained with our visual systems (Ruiz, 1999).

3.4.1. Radicchio Harvesting

Through laboratory tests, a viability study of the system was achieved along with field validation of the vision-based module. A prototype functioning in a testbed simulating quasi-real working conditions was used for the laboratory experiments. To optimize and set up components of the system, this stage was helpful. Then, in the field tests, the performance of the RVL module was authorized. The connection between the two four-bar linkages is provided by the three 3 mm thick steel plates as shown in Fig.3 12 consisting of 2 mm thick and 20 mm diameter aluminum tubes, between the carrier and the manipulator, and between the gripper and the manipulator. All the revolute joints are DryLin® bushings. At the end of the manipulator, a preliminary two-finger gripper was mounted. Without the gripper, the overall weight of the robotic arm is about 25 kg. Figure 3.12(b) shows the sparse fist-size rocks and the laboratory testbed set with characteristic agricultural terrain (Zheljazkov et al., 2013).

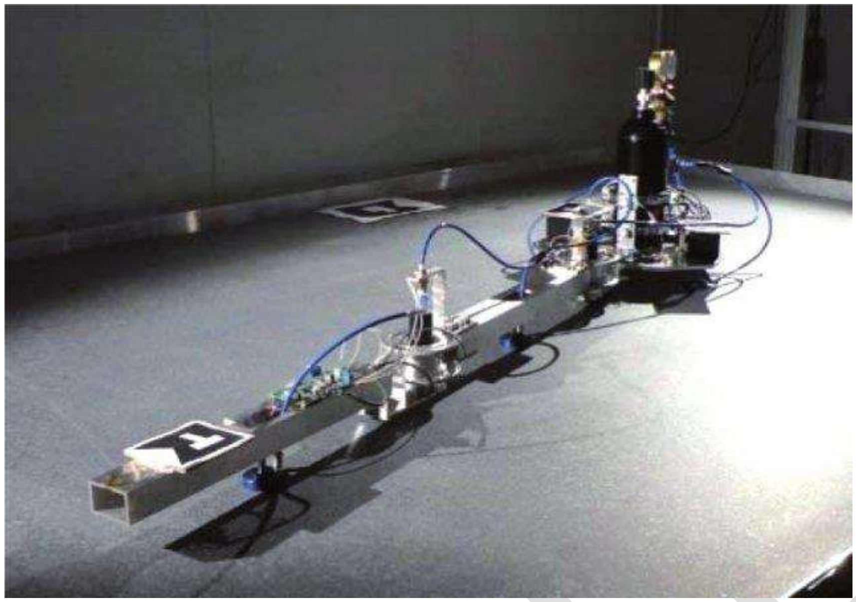

Figure 3.12. The robotic harvester prototype operating in the laboratory testbed

[Source: https://www.researchgate.net/figure/2-DOF-manipulator-prototype-test-bed-1_fig4_285801344]

3.4.2. Laboratory Tests

To assess the performance of the robotic harvester, a set of experiments was performed in picking up and identifying radicchios that were located randomly along the harvesting line. By the RVL module, the plant position was derived (Hatami et al., 2017).

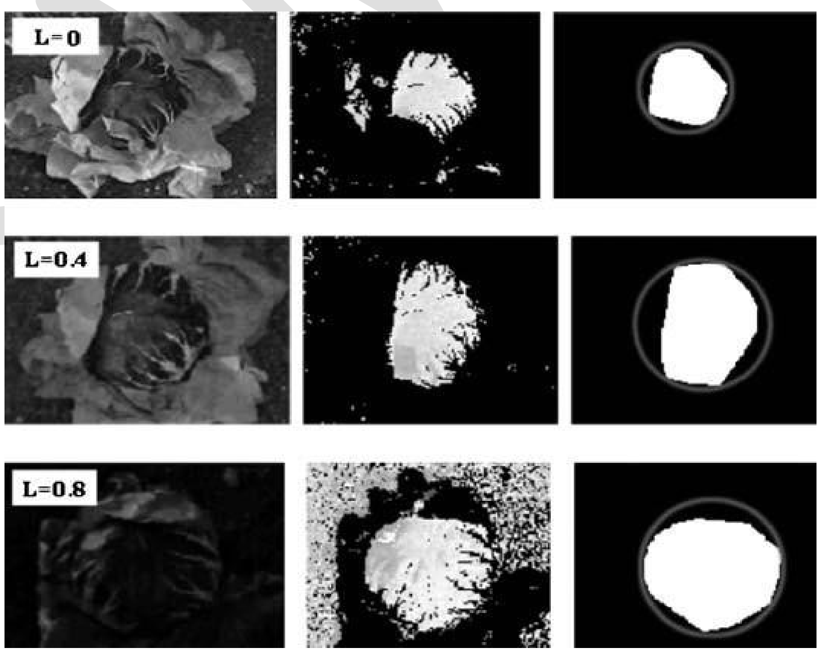

Figure 3.13. Lighting influence on the RVL module

[Source: https://link.springer.com/chapter/10.1007%2F978-3-540-74027-8_27]

The robustness of the algorithm to change in the lighting was also tested. The result of image segmentation is shown in Figure 3.13 under three dissimilar lighting circumstances attained by an adjustable video light. Even with a reduction of the environmental illumination level, the RVL works very well as much as 80% of the optimal value ($L = 0.8$), as shown in the bottom image of Fig.3 13.

3.4.3. Fennel Cutting

A laboratory testbed was set up, to test the performance of the FVI system using a ground-fixed firewire camera directing straight down 1 m across from a 2 m×0.8 m conveyor, simulating a characteristic post-harvest environment. To detect the leaf and root part of 30 cm lengthy fennel plants roaming on the conveyor with random alignment at the speediness of about 1.5 m/s, the FVI was extensively tested (Bell et al., 2008).

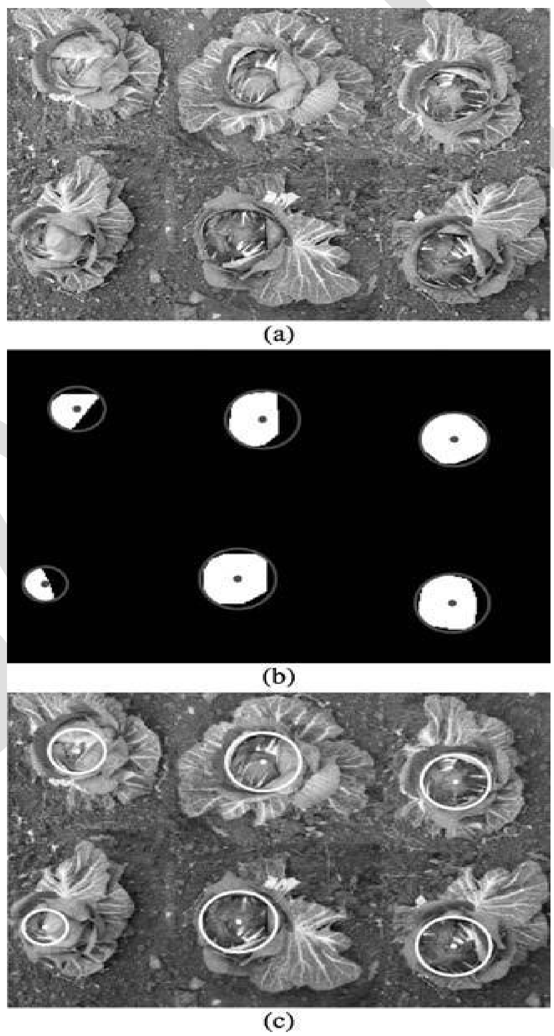

Figure 3.14. Plant detection in the field: acquired image (a), plant thresholding (b), and radicchio localization (c)

[Source: https://link.springer.com/chapter/10.1007%2F978-3-540-74027-8_27]

The color filtering-based approach was adopted, in experiments of Foglia et al. (2006) to approximate the orientation of the plants. The lines of cutting for all the plants were set correctly by the system for a typical measurement as shown in Fig.3 15. In the experiments, no false detection was observed. The effect of lighting conditions on the performances on the FVI system was detected.

In Fig.3 16, the results are gathered showing good robustness and having a light reduction as much as 50% of the optimum value (L = 0.5). Though, for this application, lighting is predictable not to be a serious factor, as post-harvesting processes are usually achieved in structured

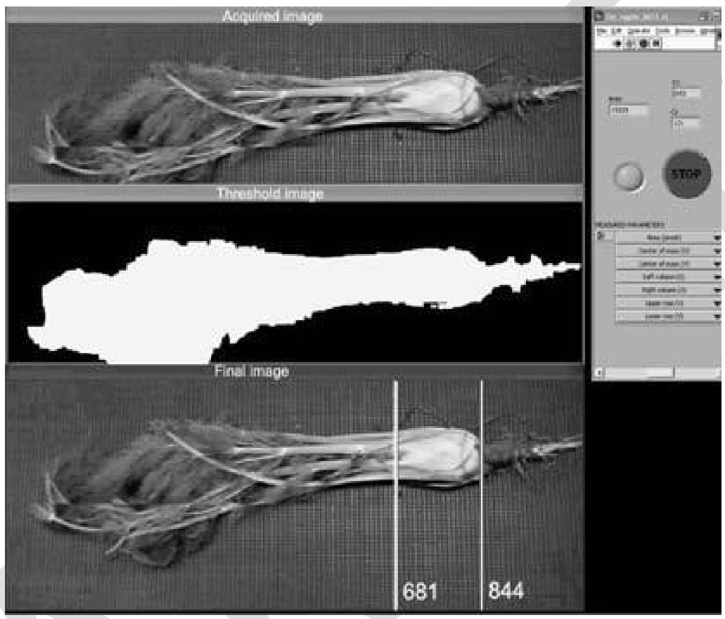

Figure 3.15. The typical measurement obtained from the FVI module

[Source: https://link.springer.com/chapter/10.1007%2F978-3-540-74027-8_27]

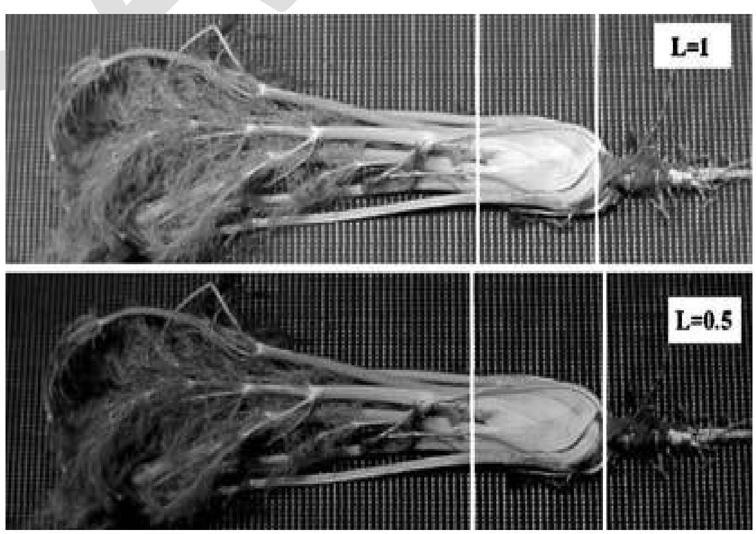

Figure 3.16. Lighting influence on the FVI module

[Source: https://link.springer.com/chapter/10.1007%2F978-3-540-74027-8_27]

environments. To estimate fennel orientation, implementing the template-based approach, experiments have also been accomplished; the cutting lines for this case are detected correctly by the FVI for only 80% of the plants. The differences in dimension and shape between plants are the cause of the lower performance, which is not accounted for in the template-based approach (Al-Dalain et al., 2012).

References

Ahmed, M. F., Zayan, A. S., & Rashed, M. S. (2016). Evaluation of seed coating with certain bio-agents against damping-off and root rot diseases of fennel under organic farming system. *J. Phytopathol. Pst. Mgmt*, *3*, 11-23.

Al-Dalain, S. A., Abdel-Ghani, A. H., Al-Dala'een, J. A., & Thalaen, H. A. (2012). Effect of planting date and spacing on growth and yield of fennel (Foeniculum vulgare Mill.) under irrigated conditions. *Pak J Biol Sci*, *15*(23), 1126-32.

Antonelli, M. G., Zobel, P. B., Durante, F., & Raparelli, T. (2017). Development of an automated system for the selective harvesting of radicchio. *International Journal of Automation Technology*, *11*(3), 415-424.

Anubhuti, P., Rahul, S., & Kant, K. C. (2011). Standardization of fennel (Foeniculum vulgare), its oleoresin and marketed ayurvedic dosage forms. *International Journal of Pharm Sci and Drug Res*, *3*(3), 265-269.

Arima, S., Kondo, N. and Monta, M. (2004). Strawberry Harvesting Robot on Tabletop Culture. ASAE Paper no. 04-3089, pp. 1-30. St. Joseph, Mich., ASAE.

Artés, F., Escalona, V. H., & Artés-Hdez, F. (2002). Modified atmosphere packaging of fennel. *Journal of food science*, *67*(4), 1550-1554.

ASAE Paper no. 04-3083, pp. 1-20. St. Joseph, Mich., ASAE.

Bell, C. E., Easley, T., & Goodman, K. R. (2008). Effective fennel (Foeniculum vulgare) control with herbicides in natural habitats in California. *Invasive Plant Science and Management*, *1*(1), 66-72.

Benson, E., Reid, J., Zhang, Q. (2003). Machine Vision–Based Guidance System for an Agricultural Small-Grain Harvester. Trans. of the ASAE, Vol. 46(4), 1255–1264.

Brown, G.K. (2002). Mechanical harvesting systems for the Florida citrus juice industry. ASAE Paper no. 02-1108, pp. 1-30. St. Joseph, Mich., ASAE.

Chi, Y.T., and Ling, P. (2004). Fast Fruit Identification for Robot Tomato Picker. ASAE Paper no. 04-3083, pp. 1-20. St. Joseph, Mich., ASAE.

Dobrusin, Y., Edan, Y., Grinshpun J., Peiper U.M., and Hetzroni A. (1992). Realtime image processing for robotic melon harvesting. ASAE Paper No. 92-3515, pp. 1-43. St. Joseph, Mich., ASAE.

Doeney D., Gilles D.K., and Slaughter D. (2003). Ground based vision identification for weed mapping using DPGS. ASAE Paper no. 03-1005, pp. 5-23. St. Joseph, Mich., ASAE.

Edan T., Rogozin D., Flash T., and Miles G. E. (2000). Robotic Melon Harvesting. IEEE Trans. on Robotics and Automation, Vol. 16 (6), 831–834.

Escalona, V. H., Artés-Hernández, F., & Artés, F. (2005). Gas composition and temperature affect quality of fresh-cut fennel. *HortScience*, *40*(3), 737-739.

Foglia, M. M., Gentile, A., & Reina, G. (2008). Robotics for agricultural systems. In *Mechatronics and Machine Vision in Practice* (Vol.1, pp. 313-332). Springer, Berlin, Heidelberg.

Foglia, M., and Reina, G. (2006), "Agricultural Robot for Radicchio Harvesting," Journal of Field Robotics, Vol. 23, Nos 6/7.

Foglia, M., Gentile, A., & Reina, G. (2005). A vision-based cutting system for fennel post-harvest processing. *Proc. of XVII AIMETA, Firenze, Italy*, 1, 11-15.

Gao, F. S., & Wang, M. Y. (2011). Breeding of a High Yield and Quality Fennel Variety'Denong No. 1'with Cutting Tolerance. *Northern Horticulture*, *2011*(22), 73.

Hannan, M.W., and Burks, T. (2004). Current Developments in Automated Citrus Harvesting. ASAE Paper no. 04-3087, pp. 1-22. St. Joseph, Mich., ASAE.

Hatami, T., Johner, J. C. F., & Meireles, M. A. A. (2017). Investigating the effects of grinding time and grinding load on content of terpenes in extract from fennel obtained by supercritical fluid extraction. *Industrial crops and products*, *109*, 85-91.

Humburg, D.S. and Reid, J.F. (1992). Field performance of machine vision for the selective harvest of green asparagus. Trans ASAE, 100(2), 81–92.

Jeon, H. Y., L.F. Tian and T. Grift. (2005). Developmnent of an individual weed treatment system using a robotic arm. ASAE Paper no. 05-1004 pp. 1-32. St. Joseph, Mich., ASAE.

KELC, D., VINDIŠ, P., RAKUN, J., STAJNKO, D., & LAKOTA, M. (2019). TECHNOLOGY FOR A 'BABY LEAF'PRODUCTION OF A CORN SALAD AND RADICCHIO. In *Proceedings of the 47th International Symposium, Actual Tasks on Agricultural Engineering, 5-7 March 2019, Opatija, Croatia* (Vol.1, pp. 251-258). University of Zagreb, Faculty of Agriculture.

Kondo, N., and Ting, K. (1998). Robotics for Bioproduction Systems. St. Joseph, Mi. ASAE, Vol.1, pp. 1-30.

Ling, P., Ehsani, R., Ting, K., Yu-Tseh Chi, Ramalingam, N., Klingman, M., Draper, C. (2004). Sensing and End-Effector for a Robotic Tomato Harvester. ASAE Paper no. 04-3088 pp. 1-21. St. Joseph, Mich., ASAE.

Masuhr, T., & Menzel, R. (1972). Learning experiments on the use of side—specific information in the olfactory and visual system in the honey bee (Apis mellifica). In *Information Processing in the Visual Systems of Anthropods* (Vol.1, pp. 315-321). Springer, Berlin, Heidelberg.

Milella, A., Reina, G., & Foglia, M. (2006). Computer vision technology for agricultural robotics. *Sensor Review*, *26*(4), 290-300.

Milella, A., Reina, G., Foglia, M. (2006). Computer Vision Technology for Agricultural Robotics. Sensor Review, Vol. 26(4), pp. 1-30.

Milella, A., Reina, G., Foglia, M., & Gentile, A. (2004). Computer vision applications in agricultural robotics. In *11th IEEE International Conference on Mechatronics and Machine Vision in Practice (Vol.11, pp. 1-33)*.

Monta, M., Kondo, N., and Ting, K.C. (1998). End-effector for Tomato Harvesting Robot. Artificial Intelligence Review. 12, 11–25.

Monta, M., Kondo, N., Shibano, Y., Mohri, K., Yamashita, J., and Fujiura, T. (1992). Agricultural Robots (3), Grape Berry Thinning Hand. ASAE Paper No. 92-3519, pp. 1-34. St. Joseph, Mich., ASAE.

Murakami, N., Inoue, K., and Otsuka, K. (1995). Selective Harvesting Robot for Cabbages. In Proc. of Int. Symposium of Automation and Robotics in Bio-production and Processing. JSAM, 2, 24–31.

Nagata, M., and Cao, Q. (1998). Study on Grade Judgment of Fruit Vegetables Using Machine Vision. Japan Agricultural Research Quarterly, 32 (4), 1-55.

Peterson, D. L. and Wolford, D. (2003b). Fresh–Market Quality Tree Fruit Harvester Part II, Apples. Applied Engineering in Agriculture. 19(5), 545–548.

Peterson, D. L., Whiting, D., and Wolford, S. D. (2003a). Fresh–Market Quality Tree Fruit Harvester Part I, Sweet Cherry. Applied Engineering in Agriculture. 19(5), 539–543.

Pilarski, T., Happold, M., Pangels, H., Ollis, M., Fitzpatrick, K., and Stentz, A. (1999). The Demeter System for Automated Harvesting. In Proc. of the 8th Int. Topical Meeting on Robotics and Remote Systems, Vol.8, pp. 10-44.

Ruiz, L. (1999). Fennel (Faeniculum vulgare) and Native Species. *Examining a long term study on exotic species management methods and experiments on the basic establishment requirements of native species. Senior Thesis. Board of Environmental Studies, University of California, Santa Cruz, 1, 1-33*.

Sacchetti, G., Appendino, G., Ballero, M., Loy, C., & Poli, F. (2003). Vittae fluorescence as a tool to differentiate between poisonous and non-poisonous populations of giant fennel (Ferula communis) of the island Sardinia (Italy). *Biochemical Systematics and Ecology*, *31*(5), 527-534.

Sciavicco, L., and Siciliano B.. (2000). Modelling and Control of Robot Manipulators. London, Springer-Verlag, 1, 1-42.

Solis-Salazar, M., González-Lutz, M. I., Mora-Acedo, D., & Duran-Quiros, A. (2008). Radicchio (Cichorium intybus) for export: variety evaluation, size of seedlings for transplant and the use of a soil plastic cover. *Agronomía Mesoamericana*, *19*(2), 271-278.

Van Henten, E.J., Hemming, J., Van Tuyl, B.A.J., Kornet J.G., Meuleman J., Bontsema J., Van Os E.A. (2002). An autonomous robot for harvesting cucumbers in greenhouses. Autonomous Robots, 13, 241–258.

Xu S., Freund, R., and Sun, J. (2003). Solution Methodologies for the Smallest Enclosing Circle Problem. Journal of Computational Optimization and Applications, 25, 283–292.

Zheljazkov, V. D., Horgan, T., Astatkie, T., & Schlegel, V. (2013). Distillation time modifies essential oil yield, composition, and antioxidant capacity of fennel (Foeniculum vulgare Mill). *Journal of oleo science*, *62*(9), 665-672.

Zion, B., Mann, M., Levin, D., Shilo, A., Rubinstein, D., & Shmulevich, I. (2014). Harvest-order planning for a multiarm robotic harvester. *Computers and Electronics in Agriculture*, *103*, 75-81.